

## ORIGINAL ARTICLE OPEN ACCESS

# 3D Method for the Volumetric Evaluation and Visualisation of Dental Biofilms: A Proof-of-Principle Study

Katja Povšič<sup>1,2</sup>  | Haris Munjaković<sup>1,2</sup>  | Vanja Erčulj<sup>3</sup> | Aleš Fidler<sup>4,5</sup> | Rok Gašperšič<sup>1,2</sup>

<sup>1</sup>Department of Oral Medicine and Periodontology, Faculty of Medicine, University of Ljubljana, Ljubljana, Slovenia | <sup>2</sup>Department of Oral Medicine and Periodontology, University Medical Centre Ljubljana, Ljubljana, Slovenia | <sup>3</sup>Rho Sigma Research & Statistics, Ljubljana, Slovenia | <sup>4</sup>Department of Endodontics and Operative Dentistry, Faculty of Medicine, University of Ljubljana, Ljubljana, Slovenia | <sup>5</sup>Department of Restorative Dentistry and Endodontics, University Medical Centre Ljubljana, Ljubljana, Slovenia

**Correspondence:** Katja Povšič ([katja.povsic@kclj.si](mailto:katja.povsic@kclj.si))

**Received:** 1 February 2025 | **Revised:** 27 July 2025 | **Accepted:** 7 August 2025

**Funding:** This work was supported by the Ministry of Higher Education, Science and Innovation, Republic of Slovenia, P3-0293.

**Keywords:** computer-assisted image analysis | dental plaque | dental plaque index | diagnostic imaging | digital technology | three-dimensional imaging

## ABSTRACT

**Background and Objective:** Traditional and planimetric plaque indices rely on plaque-disclosing agents and cannot quantify three-dimensional (3D) structures of dental biofilms. We introduce a novel computer-assisted method for evaluating and visualising plaque volume using intraoral scans (IOSs).

**Materials and Methods:** This was a 4-day, non-brushing, plaque-regrowth study ( $n = 15$ ). All plaque was removed at baseline (T0). IOSs at T0 and after 4 days (T4) were used for volumetric plaque assessment in six steps: model acquisition, model superimposition, computer-aided determination of tooth-surface margins, tooth-surface superimposition, visualisation and volumetric evaluation of biofilms. Plaque formation at T4 was additionally assessed with the Turesky Modification of the Quigley–Hein Plaque Index (TMQHPII). We used Pearson's correlation coefficients and multilevel models to investigate the relationships between TMQHPII, volumetric plaque index (VPI) and the adjusted volumetric plaque index (AVPI, plaque volume/area).

**Results:** VPI and AVPI positively correlated with the TMQHPII, showing higher variability at lower TMQHPII scores. VPI had a lower threshold for plaque detection and higher sensitivity than the TMQHPII. VPI and TMQHPII were highest on vestibular, maxillary and molar surfaces.

**Conclusion:** VPI quantifies biofilm deposits, is a more precise measure for plaque detection than the TMQHPII and can be visualised using colour-coded maps displaying areas of equal plaque thickness.

## 1 | Introduction

Dental biofilms comprise a complex community of microorganisms in an extracellular polymeric matrix (Jakubovics et al. 2021). Biofilm accumulation is usually evaluated visually using plaque-disclosing agents (PDAs) (Fasoulas et al. 2019), usually with the Turesky Modification of the Quigley–Hein Plaque Index (TMQHPII) (Lobene et al. 1982; Turesky et al. 1970). However, its diagnostic accuracy is low because of

intra-/inter-examiner variability and subjectiveness, imprecision at low/high plaque levels and unequal increments between scores (La Rosa et al. 2023).

New imaging methods have the potential to overcome the shortcomings of traditional plaque scoring indices (TPSIs). Fluorescence-based and planimetric approaches to conventional digital photographs and/or intraoral scans (IOSs) have already been investigated (Del Rey et al. 2023; La Rosa

This is an open access article under the terms of the [Creative Commons Attribution-NonCommercial-NoDerivs](https://creativecommons.org/licenses/by-nc-nd/4.0/) License, which permits use and distribution in any medium, provided the original work is properly cited, the use is non-commercial and no modifications or adaptations are made.

© 2025 The Author(s). *Journal of Clinical Periodontology* published by John Wiley & Sons Ltd.

et al. 2023). However, these methods (except for quantitative light-induced fluorescence) still rely on PDAs (Doi et al. 2021; Giese-Kraft et al. 2022; Jung et al. 2022) and do not utilise the full potential of three-dimensional (3D) data. Furthermore, no method has quantified the volume or thickness of dental biofilm deposits.

The present study aimed to introduce a novel computer-aided method for the volumetric evaluation and visualisation of changes in dental biofilms using IOSs and compare it with TMQHPII. We presumed that the volumetric assessment of dental biofilms would demonstrate greater sensitivity than TMQHPII due to a lower threshold for plaque detection.

## 2 | Materials and Methods

The study was performed from January to February 2023 at the University Dental Clinic of Ljubljana, Slovenia. It was approved by the National Medical Ethic Committee (0120-444/2022/3) and registered at [ClinTrials.gov](https://www.clinicaltrials.gov) (NCT05709015). All subjects signed informed consent forms. The study followed the principles of the Declaration of Helsinki.

### 2.1 | Design

The study was designed as a 4-day non-brushing plaque-regrowth model (Addy et al. 1983). Healthy consecutively selected volunteers without periodontal pathologies were included according to an inclusion/exclusion criterion (Table S1). During the 4-day test interval, subjects stopped all mechanical/chemical oral hygiene. A clinical examination and IOS were performed (K.P.) at the beginning and end of the study.

### 2.2 | Clinical Protocol

At baseline (T0), subjects received a 30-min full-mouth supragingival dental prophylaxis with piezoelectric ultrasonic instruments (PiezoLED ultrasonic scaler, Piezo-Scaler tip-203; KaVo dental, Biberach, Germany) and tooth polishing using prophylactic bristle brushes and polishing paste (Proxyt RDA-7; Ivocal Vivadent, Schaan, Liechtenstein) until all plaque/stain/calculus was removed. Interdental spaces were cleaned with floss (Essential-Floss, Super-Floss; Oral-B, Kronberg, Germany). Next, IOSs were obtained in the high-resolution mode (Schmidt et al. 2022) using intraoral optical scanning (Trios 4; 3shape, Copenhagen, Denmark). Subjects were then instructed to stop all mechanical/chemical oral hygiene practices for four consecutive days and follow their normal diet.

A follow-up was performed after 4 days (T4). IOSs were obtained first, followed by the application of a two-tone PDA containing the dyes CI 42090 and 45410 (Curaprox PlaqueFinder-260 disclosing solution; Curaden, Kriens, Switzerland) using cotton pellets. Participants were then asked to rinse their oral cavities with 20 mL of distilled water for 15 s. New plaque formation was evaluated using the TMQHPII scores 1–5 independently at six sites per tooth, excluding third molars. TMQHPII was assessed

(K.P.) after calibration (Figure S1) for dark (blue/purple) disclosed plaque (DDP) and total (pink + blue/purple) disclosed plaque (TDP) (Volgenant et al. 2016). Finally, the subjects received supragingival dental prophylaxis and tooth polishing, followed by topical application of fluorides (Elmex Gelee 1.25% dental gel; CP GABA GmbH, Hamburg, Germany).

### 2.3 | Digital Volumetric Plaque Analysis

The volumetric plaque analysis was performed (K.P.) in six steps (Figure 1): digital model acquisition, model superimposition, computer-aided determination of tooth surface margins on vestibular and oral surfaces of each tooth (defined as regions of interest ROIs), superimposition of tooth surfaces (i.e., ROIs), visualisation and volumetric evaluation of dental biofilm. Changes in surface topography between T0 and T4 were assessed separately for each tooth surface pair. The deviation ( $d$ ) values were defined as the ‘thickness’ with regard to the ROI at T0. The surface area ( $s$ ) was also calculated as a function of the ROI at T0. Using an automated surface comparison tool, the ‘volume’ was subsequently calculated in terms of the integrated distance using the following formula:

$$\text{Integrated distance} = \sum d \times s_i$$

The volumetric plaque index (VPI, in  $\text{mm}^3$ ), that is, the volume of dental plaque accumulated at T4 with reference to T0, was mathematically defined as the positive value of the ‘volume’ calculated above (i.e., positive value of the integrated distance) using the following formula:

$$\begin{aligned} \text{Integrated abs distance} - |\text{negative values}| = \\ \text{Integrated abs distance} - \frac{(\text{Integrated abs distance} - \text{Integrated distance})}{2} \\ = \text{positive values} = \text{VPI} \end{aligned}$$

Since teeth vary in shapes/sizes, the volume of plaque was standardised per individual tooth surface area, that is, the ROI. The adjusted volumetric plaque index (AVPI) was expressed in  $\text{mm}^3/\text{mm}^2$  (which should not be interpreted as a weighted average of plaque thickness) as

$$\text{AVPI} = \frac{\text{VPI}}{\text{ROI surface area}}$$

### 2.4 | Calibration of Volumetric Analysis

An ex vivo validation protocol using a dental study model was devised to assess the accuracy and precision of the volumetric analysis. Intraoral (Trios 4; 3shape, Copenhagen, Denmark) and extraoral scans (Medit T300, Medit, Seoul, Korea) of the model were obtained at baseline and after 4 days of suspension in a liquid medium, inoculated with supragingival biofilm, to compare differences in plaque accumulation. An extraoral scanner was selected as a reference since it is more accurate than intraoral scanners for whole-arch scanning (Lee et al. 2020). Furthermore, an intra-operator calibration exercise was performed to assess the repeatability of the volumetric analysis. Both protocols are described in Figure S2.

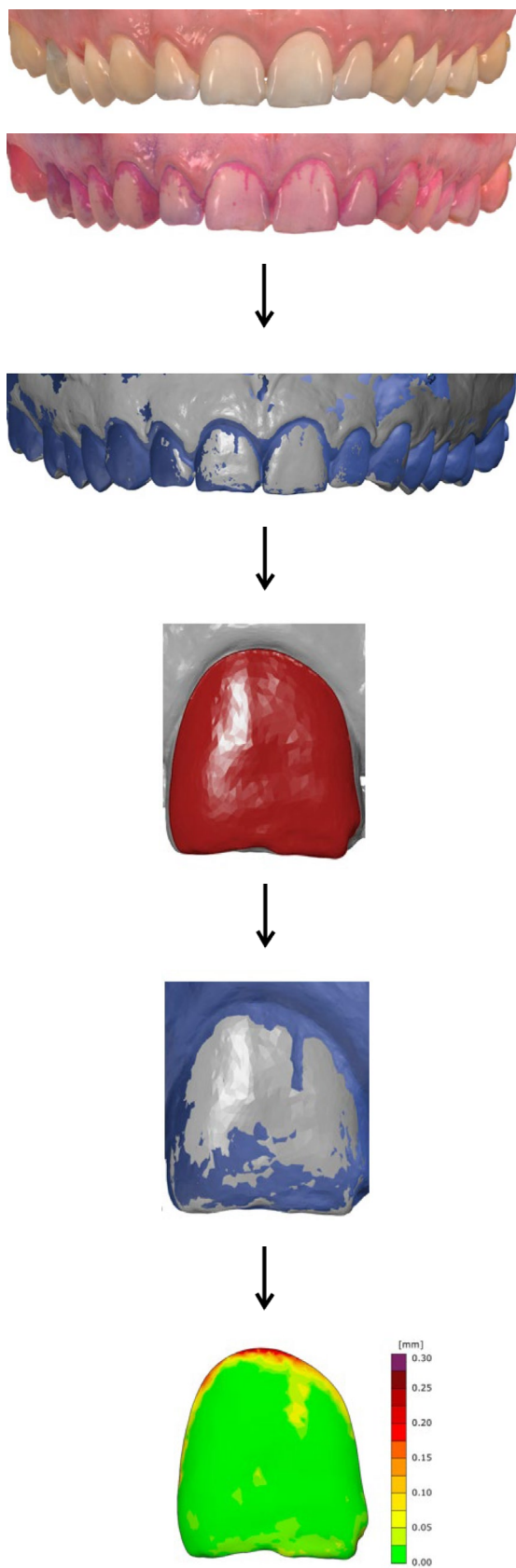


**FIGURE 1** | Workflow of the digital volumetric plaque analysis.

### Digital model acquisition

IOS were obtained with an intraoral optical scanner using a standard scanning strategy (Kuralt et al., 2020) at T0 (image above) and T4 (image below). 3D models were exported in the Standard Tessellation Language (.stl) format.

### Digital model superimposition

Post-processing was performed using GOM Inspect 2022 (GOM GmbH, Braunschweig, Germany) with the iterative closest point algorithm (Besl & McKay, 1992). Initial alignments of each digital model pair (T0–T4) was performed with the automated Prealignment tool using whole models (soft tissues and teeth) to superimpose the datasets. Initial alignments were prerequisites for further alignments.

### Computer aided determination of tooth surface margins

Regions of interest (ROIs), i.e. the vestibular/oral surfaces of each tooth, were delineated on T0 models. Their margins were manually defined with landmark curves using the Maximum curvature function of the Surface Curve tool, with 5–10 points snapping to the clicked position at the gingival margin and the incisal/occlusal edge on the surface of the model (Kuralt & Fidler, 2022). The mesial/distal margins of the ROIs were determined by the software with automated detection of the maximal surface curvature, thus connecting the manually defined landmark curves at the gingival margin and incisal/occlusal edge.

### Superimposition of tooth surfaces

Each ROI created on the T0 scan was individually aligned with the corresponding tooth surface on the T4 model using the automated Local Best-Fit tool (Kuralt & Fidler, 2021). The deviation of the alignment with respect to the ROI was defined as the mean absolute distance of the points of the actual mesh to the specified CAD (Vág et al., 2019).

### Visualisation and volumetric evaluation of dental biofilm

Changes in surface topography between each ROI pair (T0–T4) were visualised using the Surface comparison tool: colour scale deviations defining the difference between the two were used to calculate the volume of accumulated plaque

The clinical applicability of the method was assessed in an in vivo validation trial to evaluate volumetric changes specifically related to plaque accumulation and its subsequent removal (Figure S3).

## 2.5 | Statistical Analysis

The a priori sample size could not be determined in advance because no prior data exists regarding dental plaque volume. A convenience sample of 15 subjects was chosen (Gkavela et al. 2024). The sample size was increased by 10% to account for potential dropouts. An additional sample size calculation based on the study's primary objective (comparison between the VPI and TMQHPII for TDP) was performed post hoc for a two-tailed test using the Fisher Z-transformation of Pearson's  $r$ :

$$n = \left( \frac{Z_{1-\alpha/2} + Z_{1-\beta}}{0.5 \times \ln\left(\frac{1+r_1}{1-r_1}\right) - 0.5 \times \ln\left(\frac{1+r_0}{1-r_0}\right)} \right)^2 + 3$$

At  $r_0 = 0$ ,  $r_1 = 0.66$ ,  $\alpha = 0.05$  and  $\beta = 0.2$ , the sample size was calculated to be 15 subjects (MedCalc v. 23.3.2; MedCalc Software Ltd., Ostend, Belgium). The statistical power of the correlations between the VPI/AVPI and the TMQHPII was also determined post hoc.

VPI and AVPI were described with means and standard deviations (SD). Distribution normality was assessed using the Shapiro–Wilk test. SDs were calculated by taking into account the nesting of measured values within tooth surfaces (i.e., ROIs), jaws and individuals. Multilevel models with random intercepts were used to test for differences between tooth surfaces, jaws and tooth types for both VPI and AVPI to account for data nesting

(site–tooth–individual). Pearson's correlation coefficient was used to calculate the correlation between the mean VPI/AVPI and the mean TMQHPII (average of three scores per tooth surface). The Kruskal–Wallis test was used to evaluate differences in VPI and AVPI between rounded averaged TMQHPII scores at the level of individual tooth surfaces. Multilevel models were used to explore the relationship between VPI, AVPI and TMQHPII. The Mann–Whitney U test was used for exploratory pairwise comparisons between DDP/TDP scores (as assessed using the TMQHPII) for VPI and AVPI. Intra-examiner reliability of TMQHPII was assessed using Cohen's kappa. Intra-examiner reliability of VPI was assessed using the interclass correlation coefficient (ICC). Wilcoxon's signed-rank test was employed for the comparison of intraoral and extraoral scans. Sensitivity, specificity and accuracy were calculated using TMQHPII and VPI as the diagnostic reference standards for plaque detection. Statistical significance was set at  $\alpha = 0.05$ . GRRAS guidelines (Table S2) for reporting reliability and agreement (Kottner et al. 2011) were followed. Other than the post hoc power calculation, all analyses were performed in SPSS v. 26 (IBM, Armonk, New York, USA).

## 3 | Results

### 3.1 | Study Population

Sixteen subjects were selected for inclusion; one dropped out on day 3 (personal reasons). The final sample comprised seven males and eight females (mean age: 25.25 years). One subject had a deciduous second upper right molar, which was excluded from analysis. One subject presented a case of maxillary lateral incisors aplasia, which was excluded from statistical analyses. In total, 834 tooth surfaces were analysed. In agreement with the inclusion criteria, the average number of teeth, TMQHPII

**TABLE 1** | Mean TMQHPII scores and standard deviations after 4 days.

	Full mouth		
TDP (mean [SD])	2.49 (0.31)		
DDP (mean [SD])	0.82 (0.42)		
	Non-interdental sites	Interdental sites	<i>p</i>
TDP (mean [SD])	2.45 (0.34)	2.51 (0.31)	0.176
DDP (mean [SD])	0.78 (0.43)	0.85 (0.42)	0.142
	Vestibular sites	Oral sites	<i>p</i>
TDP (mean [SD])	2.97 (0.48)	2.01 (0.25)	<0.001*
DDP (mean [SD])	1.23 (0.56)	0.42 (0.39)	<0.001*
	Non-molars	Molars	<i>p</i>
TDP (mean [SD])	2.47 (0.34)	2.53 (0.38)	<0.001*
DDP (mean [SD])	0.82 (0.47)	0.84 (0.38)	0.364
	Maxilla	Mandible	<i>p</i>
TDP (mean [SD])	2.69 (0.31)	2.29 (0.38)	<0.001*
DDP (mean [SD])	1.18 (0.54)	0.47 (0.42)	<0.001*

Abbreviations: DDP, dark coloured disclosed plaque; SD, standard deviation; TDP, total disclosed plaque.

\*Statistical significance at  $\alpha = 0.05$ .

**TABLE 2** | VPI and AVPI (mean and standard deviation; SD) 4 days after the cessation of all mechanical and chemical oral hygiene practices.

	VPI (mm <sup>3</sup> )		AVPI (mm <sup>3</sup> /mm <sup>2</sup> )	
	Mean (SD)	<i>p</i>	Mean (SD)	<i>p</i>
All teeth	0.78 (0.52)		0.020 (0.010)	
Tooth surface		<0.001*		0.008*
Vestibular	0.94 (0.48)		0.018 (0.010)	
Oral	0.60 (0.49)		0.016 (0.012)	
Jaw		<0.001*		0.877
Mandibular	0.68 (0.44)		0.017 (0.012)	
Maxillary	0.87 (0.57)		0.017 (0.011)	
Tooth type				0.344
Incisor	0.75 (0.57)	0.001*	0.018 (0.015)	
Canine	0.88 (0.43)	0.646	0.018 (0.011)	
Premolar	0.62 (0.41)	<0.001*	0.017 (0.011)	
Molar	0.90 (0.55)		0.016 (0.008)	

Abbreviations: AVPI, adjusted volumetric plaque index; SD, standard deviation; VPI, volumetric plaque index.

\*Statistical significance at  $\alpha = 0.05$ .

and probing pocket depth were 29.7 teeth (SD = 0.9 teeth), 8.6% (SD = 4.1%) and 2.7 mm (SD = 0.4 mm), respectively.

### 3.2 | Visual Evaluation

The calibration exercise for TMQHPII yielded Cohen's kappa = 0.82 and 95% confidence interval (CI): 0.71–0.90. Mean TMQHPII full-mouth scores at T4 are shown in Table 1. Significantly higher plaque scores ( $p < 0.001$ ) were observed at vestibular and maxillary sites for both TDP and DDP and at molars for TDP.

### 3.3 | Digital Evaluation

The means of the VPI and AVPI at T4 are shown in Table 2. Plaque volume differed significantly between tooth surfaces, types and jaws. VPI was greater on vestibular surfaces ( $p < 0.001$ ), molars compared to incisors ( $p = 0.001$ ) and canines ( $p < 0.001$ ) and in the maxilla ( $p < 0.001$ ). After adjustment, plaque volume remained significantly greater on vestibular surfaces ( $p = 0.008$ ) and did not differ with regard to tooth type and jaw. Colour-coded maps were used to visualise plaque thickness (Figure 2b),

showing more plaque at predilection sites. The average of the mean absolute distances at the level of all ROIs was 0.0099 mm (SD = 0.0028 mm). The average scan resolution was 27.2/mm<sup>2</sup> at the level of all whole scans and 39.2/mm<sup>2</sup> at the level of all ROIs.

The ex vivo calibration exercise showed no statistical differences (Table S3). Average VPI values from IOSs (0.61 mm<sup>3</sup>) were 0.04 mm<sup>3</sup> higher than extraoral scans (0.57 mm<sup>3</sup>). AVPI values from IOSs (0.02 mm<sup>3</sup>/mm<sup>2</sup>) were 0.01 mm<sup>3</sup> higher than extraoral scans (0.01 mm<sup>3</sup>/mm<sup>2</sup>). Accuracy was thus found to be excellent (Figure 2d,e). The VPI difference after plaque accumulation versus removal was 0.06 mm<sup>3</sup> (extraoral) and 0.05 mm<sup>3</sup> (intraoral). VPI values of consecutive extraoral scans (0.06 mm<sup>3</sup>) were 0.02 mm<sup>3</sup> lower than consecutive IOSs (0.08 mm<sup>3</sup>). AVPI averages were identical (0.00 mm<sup>3</sup>/mm<sup>2</sup>), showing high precision. The ICC for VPI was 0.98 (95% CI: 0.98–0.99). In vivo, VPI values after plaque accumulation (1.18 mm<sup>3</sup>) and removal (1.31 mm<sup>3</sup>) differed by 0.13 mm<sup>3</sup> ( $p = 0.283$ ); baseline versus post-plaque removal values differed by 0.11 mm<sup>3</sup> (Table S4).

### 3.4 | Relationship Between the TMQHPII, VPI and AVPI

Pearson's correlation coefficient showed a moderate relationship between traditional (DDP, TDP) and volumetric (VPI, AVPI) plaque indices (Table 3). The results of multilevel models showed statistically significant regression coefficients between traditional and volumetric plaque indices, with the weakest relationship being between AVPI and VPI (Table 4).

The distributions of VPI and AVPI according to the mean TMQHPII score per tooth surface (average of three scores) rounded to the nearest whole number are presented in Figure 3. VPI and AVPI distributions differed significantly between TMQHPII scores at the level of both DDP and TDP ( $p < 0.001$ ). The variability of both volumetric plaque indices was higher at lower TMQHPII scores. DDP never exceeded two-thirds of any tooth surface (no TMQHPII score 5). The outcomes of the exploratory pairwise comparisons between DDP/TDP scores for VPI and AVPI are presented in Tables S5 and S6.

When using TMQHPII as the reference, the specificity of VPI was low at the level of both TDP and DDP, while accuracy was low for DDP and high for TDP. When using VPI as the reference, the sensitivity and accuracy of TMQHPII were high at the level of TDP and low for DDP (Table S7).

## 4 | Discussion

The study introduced a novel method for the digital volumetric assessment of dental biofilms using two indices—VPI and AVPI. The main advantages of a volumetric approach included the objective assessment of plaque volume and the visualisation of plaque location using colour-coded maps showing areas of equal plaque thickness without the need for PDAs. Unlike planimetry, volumetry overcame the distortion of 3D objects on 2D surfaces and avoided the poor reproducibility of planimetric approaches due to the limited colour image quality of screenshots taken by IOSs (Jung et al. 2024).

Nevertheless, TPSIs (Rustogi et al. 1992; Silness and Løe 1964; Turesky et al. 1970) remain the gold standard for plaque assessment. TPSIs provide ordinal scales for scoring the distribution and/or location of plaque. TMQHPII is the most

widely used plaque index (La Rosa et al. 2023) and is based on a subjective visual criterion (Lobene et al. 1989). To evaluate *all* plaque, a two-tone PDA was selected in the present study because it provides thickness-dependent differential staining:

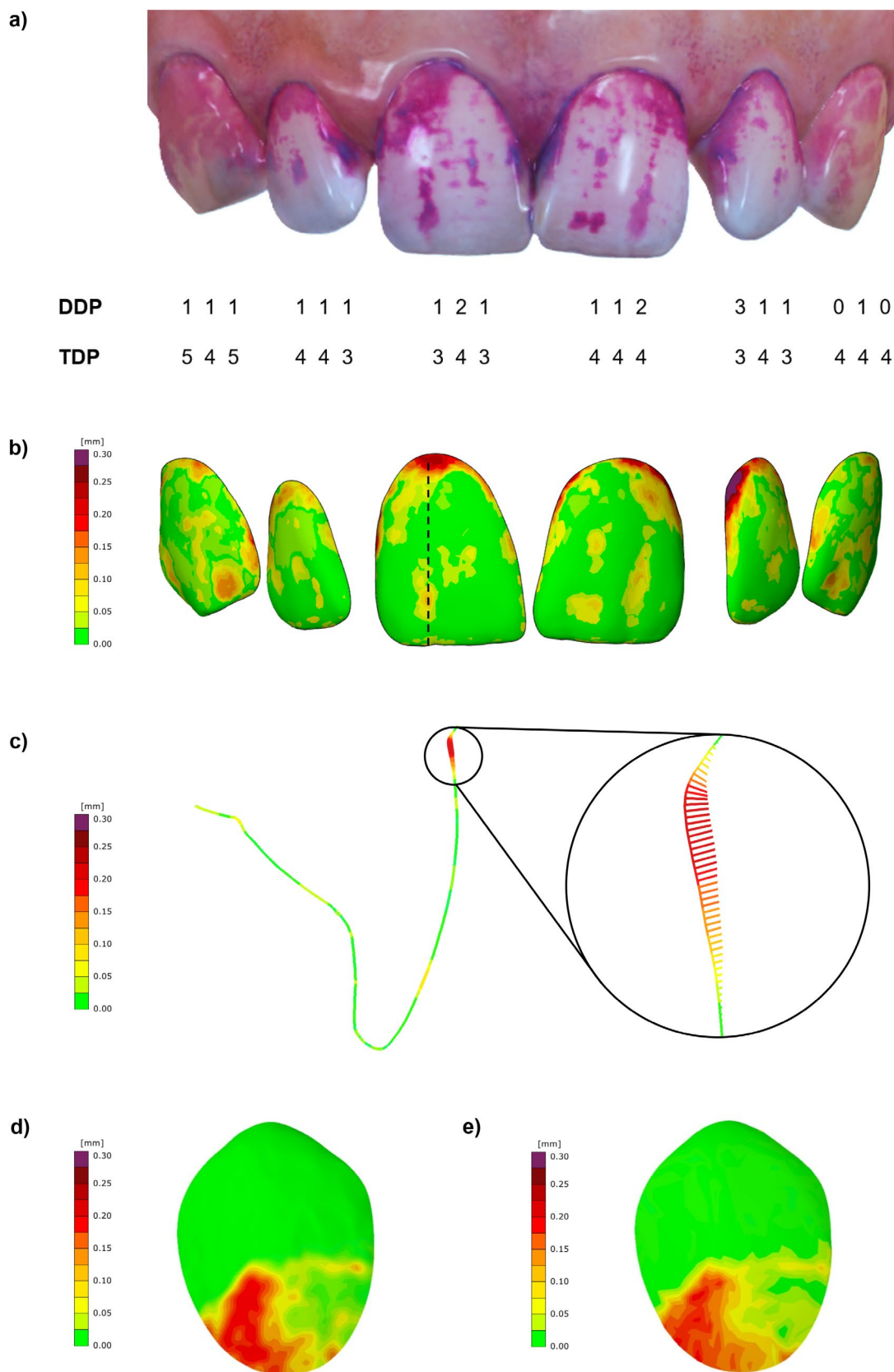


**FIGURE 2** | Legend on next page.

**FIGURE 2** | Volumetric evaluation of dental biofilm. (a) Screenshot from intraoral scan; dental biofilm was stained with a two-tone disclosing solution (Curaprox PlaqueFinder 260 disclosing solution; Curaden, Kriens, Switzerland). Plaque deposits on the buccal tooth surfaces (excluding proximal surfaces) were evaluated on three areas (distobuccal, central, mesiobuccal—separated by dotted lines) using the Turesky Modification of the Quigley–Hein plaque index (TMQHPII) for dark disclosed plaque (DDP) and total disclosed plaque (TDP). (b) Delineated buccal surfaces (reference areas) of a 3D digital model visualised using a colour-coded map of plaque thickness with discrete threshold colour ranges. The dotted line represents the location of the cross section in (c). (c) Cross section of the upper right central incisor with displayed colour-coded thickness, representing the distances between baseline and follow-up (Day 4) intraoral scans. (d, e) Volumetric evaluation of dental biofilm on a dental study model, compared between an (d) intraoral (Trios 3shape 4) and (e) extraoral (Medit T300) scanner; tooth surfaces are visualised using a colour-coded map of plaque thickness with discrete threshold colour ranges.

**TABLE 3** | Pearson's correlation coefficient between traditional and volumetric plaque index scores.

	Turesky Modification of the Quigley–Hein Plaque Index	
	TDP [ $r(1 - \beta)$ ]	DDP [ $r(1 - \beta)$ ]
VPI	0.66* (0.78)	0.62* (0.71)
AVPI	0.73* (0.89)	0.68* (0.82)

Note: The statistical power ( $1 - \beta$ ) of the correlations between VPI and AVPI in relation to the TMQHPII was determined post hoc.

Abbreviations: AVPI, adjusted volumetric plaque index; DDP, dark coloured disclosed plaque; TDP, total disclosed plaque; VPI, volumetric plaque index.

\*Statistically significant relationship ( $p < 0.001$ ).

**TABLE 4** | Comparison of regression coefficients of multilevel model analysis, with the Turesky Modification of the Quigley–Hein Plaque Index as the independent variable.

	Regression coefficient	95% confidence interval	$p$
DDP			
VPI	0.780	0.700–0.850	<0.001*
AVPI	0.002	0.001–0.003	<0.001*
TDP			
VPI	0.160	0.130–0.190	<0.001*
AVPI	0.002	0.001–0.003	<0.001*

Abbreviations: AVPI, adjusted volumetric plaque index; DDP, dark coloured disclosed plaque; TDP, total disclosed plaque; VPI, volumetric plaque index.

\*Statistical significance at  $\alpha = 0.05$ .

pink dye (supposedly ‘new plaque’) adheres to all plaque, whereas blue dye (supposedly ‘old/mature’ plaque) adheres and diffuses into denser/thicker plaque (Gallagher et al. 1977; Volgenant et al. 2016). Our results showed that the amount of DDP and TDP was lower on oral and mandibular tooth surfaces, as found by previous studies (Danser et al. 2003; Lang et al. 1973). A 4-day non-brushing model was selected because most plaque forms in the first 4 days without brushing, followed by moderate additional plaque accumulation (Dahlén et al. 1992).

VPI is an alternative plaque evaluation approach and uses superimpositions of serial 3D IOSs. It does not require a PDA, which was, in the present study, used *exclusively* to evaluate the TMQHPII. Just like TPSIs, VPI did not account for the variation

in the surface areas of individual teeth. It yielded similar outcomes as the TMQHPII in that more plaque accumulated on vestibular and maxillary sites, as well as on molars. AVPI, a measure of plaque per area, however, only showed a statistically significant difference between the volume of plaque on vestibular and oral tooth surfaces. This reflects the lower discriminatory power of standardisation (volume per area) because it reduces means and variances compared to conventional averaging (Lütkenhöner et al. 1985). This study did not limit the diet of the subjects and evaluated the natural pattern of plaque accumulation during real-life eating practices.

Digital plaque scoring systems based on (semi-)automated, computer-aided principles, such as VPI and AVPI, offer several advantages over TPSIs: acquisition of all regions (even ones inaccessible to visual examination), increased accuracy (especially area assessment, as compared to planimetric/photograph-based methods), no examiner subjectivity/variability, data archiving (La Rosa et al. 2023) and the possibility of evaluating/visualising changes with colour-coded maps (Kuralt and Fidler 2021). Colour-coded maps show plaque accumulation patterns in grooves/lingulae/valleys, accounting for the anatomical heterogeneity of teeth and (rotated) positions. Since plaque was removed from all teeth at T0, the results showed only positive changes in plaque; however, in clinical practice, volumetric changes may also be negative, indicating a reduction in plaque levels. This reverse approach, specifically related to plaque accumulation and its subsequent removal, may be more relevant for clinical practice and, as shown by the ex vivo and in vivo validation exercises, yields comparable results to the verified no-plaque/plaque sequence.

The process of volumetric plaque assessment has several limitations. Distortions during scanning often occur in posterior regions due to the scanner tip size, poor access (Abduo and Elseyoufi 2018), and shaking/movement during scanning, which affect the accuracy of model superimposition (Kihara et al. 2020). In addition, 3D model reconstruction causes larger deviations in curved areas (premolars, canines and the distal surfaces of molars) and interdental spaces, which require more captured angles during shooting (Lin et al. 2024; Winkler and Gkantidis 2020). Interdental spaces were therefore excluded from the analysis, which is one of the limitations of the study. Since scanning and superimpositions at the level of the whole digital model contribute to alignment deviations of approximately 0.1 mm (Kuralt et al. 2020), the present study performed best-fit superimpositions at the level of individual tooth surfaces, decreasing potential precision errors to approximately 0.01 mm. We can therefore not be

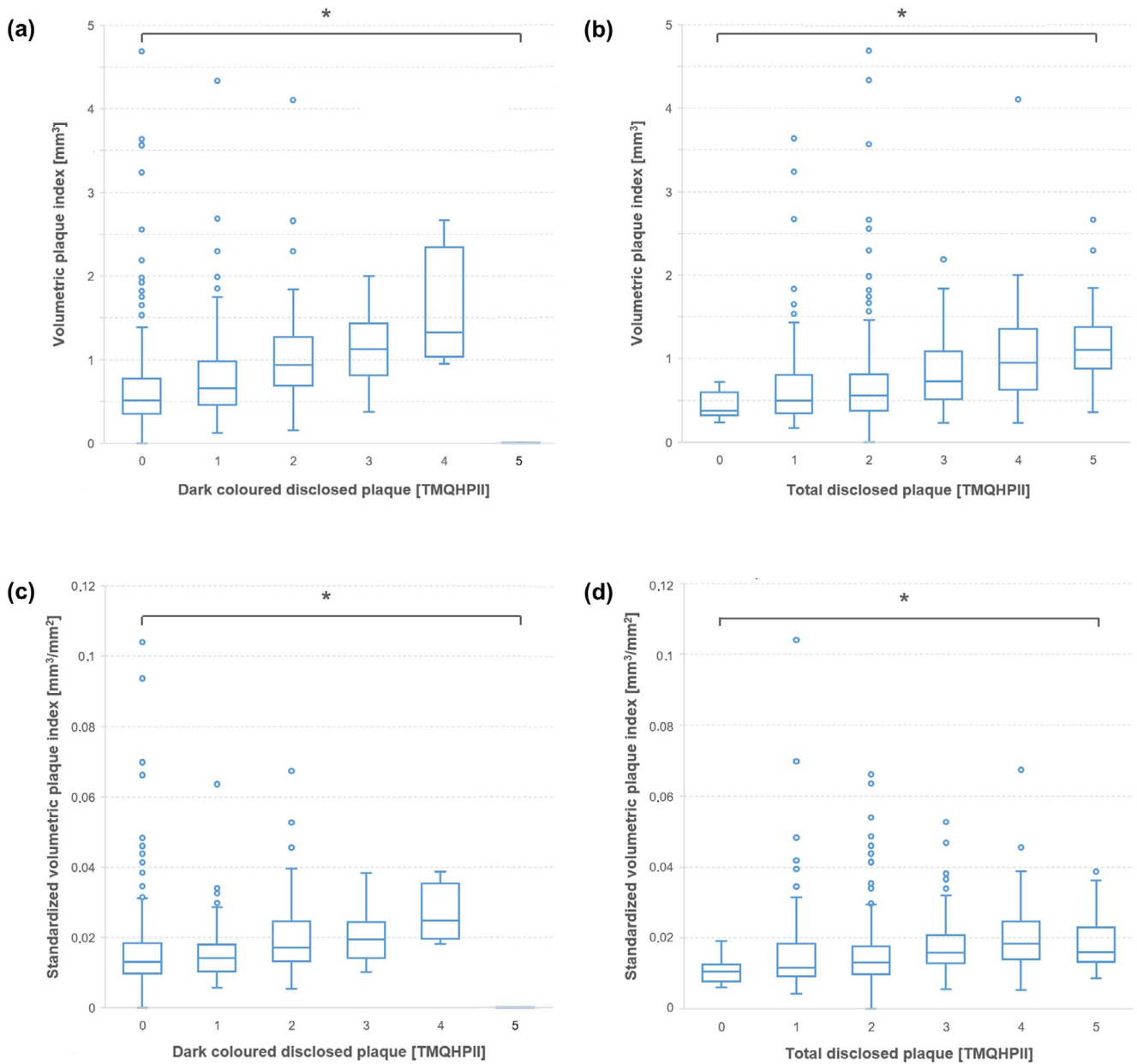


**FIGURE 3** | Agreement between the volumetric plaque index (VPI), adjusted volumetric plaque index (AVPI) and the Turesky Modification of the Quigley–Hein plaque index (TMQHPII). The values of the TMQHPII (scores 0–5) represent the average score per tooth surface (average of three scores), rounded to the nearest whole number. Relationship between (a) VPI and dark coloured disclosed plaque scores, (b) VPI and total disclosed plaque scores, (c) AVPI and dark coloured disclosed plaque scores and (d) AVPI and total disclosed plaque scores, as assessed using the TMQHPII.

certain whether plaque is present or absent up to a thickness of 0.01 mm. However, this measurement error only insignificantly contributes to the computed plaque volume due to the large variability in plaque thickness across each tooth surface. In addition, a calibration exercise assessing the volumetric differences between superimposed scans obtained from intraoral versus extraoral scans of the same object found excellent outcomes. The difference in VPI between intraoral and extraoral scans measured 0.04 mm<sup>3</sup> for plaque-covered tooth surfaces and 0.02 mm<sup>3</sup> for scan–rescan procedures, showing excellent accuracy (i.e., closeness to the true value) and precision (i.e., closeness of measurements to one another). Considering

that VPI of the subjects' tooth surfaces ranged from 0.11<sup>3</sup> to 6.12 mm<sup>3</sup>, measurement errors can be considered clinically insignificant.

The semi-automated delineation of tooth surface margins on the digital models was performed using landmark curves created by hand-picked points that snapped to their clicked positions (Kuralt and Fidler 2021; Rusinkiewicz 2004). Even though this approach to obtain VPI values shows excellent intra-operator agreement (ICC: 0.98; 95% CI: 0.98–0.99), it requires a substantial and time-consuming workload at present (10 h/patients), which is significantly more than scoring with

the TMQHPII (minutes); a higher degree of automatization and the establishment of a standardised operational framework are necessary for using VPI and AVPI in everyday clinical or research purposes (Conte et al. 2023; La Rosa et al. 2023). At present, the proposed method is at a proof-of-principle stage. Considering the rapid development of machine learning, the proposed method could be integrated into existing intraoral scanning software interfaces in the form of expansion modules, thus offering a fully automated and user-friendly experience for dentists and researchers alike, reducing the time-consuming workload to a matter of minutes needed to perform an IOS. The rationale for the volumetric analysis of dental biofilms includes objectiveness, no need for PDAs, no examiner bias, a numerical scale for statistical analysis and the possibility of comparing colour-coded maps from different timepoints. The latter comparison can expose plaque predilection sites and may be used to motivate caries-prone/periodontal/orthodontic patients in their oral hygiene practices.

The correlation coefficients between VPI/AVPI and TMQHPII indicated a moderate (Schober and Schwarte 2018) relationship, the volume of accumulated plaque increasing at higher TMQHPII scores. The differences between plaque volumes were smallest at the lower end of the TMQHPII scale, which demonstrates the exponential nature of TMQHPII and indicates that TMQHPII inadequately describes the natural development of plaque, failing to recognise plaque as a 3D object just like planimetric approaches. The variability of VPI/AVPI was also greatest at lower TMQHPII scores, which indicates unreliable staining and shows a great underestimation of higher volumes, particularly for scores 1 and 2 (both describing plaque at the gingival margin). This suggests that plaque volume at the gingival margin is often uneven and determined by site-specific variables (tooth anatomy). In addition, the gingival margin is naturally shaped as an anatomic groove itself, representing a predilection site for plaque accumulation, and exhibits thicker plaque deposits compared to the rest of the tooth due to its specific form. On the other hand, TMQHPII scores and planimetric approaches seem to be a measure of plaque location as opposed to plaque thickness, which explains the presence of outliers within each score (especially TMQHPII score 1; Figure 3). The increase in plaque volume at higher TMQHPII scores is, in turn, minimal, giving low values of the regression coefficients. Digital images (Figure 2b) emphasise small areas of thick plaque, located close to the gingival margin, while the prevailing impression by clinical visual evaluation is diffuse areas of plaque (unknown thickness) on buccal surfaces, which hamper the detection of marginal plaque quantity.

The specificity of VPI with reference to TMQHPII was very low; the former detected plaque in significantly more cases where plaque was deemed absent by the latter. Similarly, the sensitivity of TMQHPII was low for DDP when VPI was used as the reference standard; VPI detected significantly more sites with plaque deposits than TMQHPII. Both outcomes may be attributed to the lower threshold for plaque detection by VPI, which seems to be a more precise measure for plaque recognition and is able to identify plaque that is not visible to the naked eye (at a 0.01 mm limit of detection, corresponding to the size of a few bacterial cell layers; Li et al. 2015). The low values of sensitivity/specificity/accuracy emphasise the inability of TMQHPII to detect

small sub-clinical biofilm volumes and differentiate between scores 0 and 1, which puts its reputation as a gold standard under question. It is still, however, unclear which parameter (volume, thickness, location) is clinically most relevant in the maturation process of dental biofilms, thus preventing definite conclusions regarding the optimal plaque index choice.

## 5 | Conclusion

Both VPI and AVPI positively correlated with TMQHPII, offering greater objectiveness, precise and accurate volume/thickness measurements, non-invasiveness, a numerical scale and visualisation of plaque thickness using colour-coded maps without PDA application. Future longitudinal studies should monitor volumetric plaque changes in relation to its microbiological composition.

### Author Contributions

Katja Povšič contributed to conception, design, data acquisition, analysis and interpretation, and drafted and critically revised the manuscript. Haris Munjaković contributed to data acquisition and critically revised the manuscript. Vanja Erčulj contributed to data analysis and interpretation and critically revised the manuscript. Aleš Fidler contributed to data interpretation and critically revised the manuscript. Rok Gašperšič contributed to conception, design, data acquisition and interpretation, and drafted and critically revised the manuscript.

### Acknowledgements

We would like to thank our very talented dental technician, Uroš Homec, for his patience and help with extraoral scanning.

### Ethics Statement

The study was approved by the National Medical Ethic Committee of the Republic of Slovenia (0120-444/2022/3) and registered at [ClinTrials.gov](https://www.clinicaltrials.gov) (NCT05709015).

All subjects signed informed consent forms prior to inclusion in the study.

### Conflicts of Interest

The authors declare no conflicts of interest.

### Data Availability Statement

The data that support the findings of this study are available from the corresponding author upon reasonable request.

### References

- Abduo, J., and M. Elseyoufi. 2018. "Accuracy of Intraoral Scanners: A Systematic Review of Influencing Factors." *European Journal of Prosthodontics and Restorative Dentistry* 26, no. 3: 101–121. [https://doi.org/10.1922/EJPRD\\_01752ABDUO21](https://doi.org/10.1922/EJPRD_01752ABDUO21).
- Addy, M., L. Willis, and J. Moran. 1983. "Effect of Toothpaste Rinses Compared With Chlorhexidine on Plaque Formation During a 4-Day Period." *Journal of Clinical Periodontology* 10, no. 1: 89–99. <https://doi.org/10.1111/J.1600-051X.1983.TB01270.X>.
- Besl, P. J., and N. D. McKay. 1992. "A Method for Registration of 3-D Shapes." *IEEE Transactions on Pattern Analysis and Machine Intelligence* 14, no. 2: 239–256. <https://doi.org/10.1109/34.121791>.

- Conte, G., A. Amaliya, S. Gupta, et al. 2023. "Repeatability of Dental Plaque Quantitation by Light Induced Fluorescence Technology in Current, Former, and Never Smokers." *BMC Oral Health* 23, no. 1: 480. <https://doi.org/10.1186/S12903-023-03154-0>.
- Dahlén, G., J. Lindhe, K. Sato, H. Hanamura, and H. Okamoto. 1992. "The Effect of Supragingival Plaque Control on the Subgingival Microbiota in Subjects With Periodontal Disease." *Journal of Clinical Periodontology* 19, no. 10: 802–809. <https://doi.org/10.1111/J.1600-051X.1992.TB02174.X>.
- Danser, M. M., M. F. Timmerman, Y. Jzerman, M. I. Piscoer, U. V. D. Velden, and G. A. Weijden. 2003. "Plaque Removal With a Novel Manual Toothbrush (X-Active) and the Braun Oral-B 3D Plaque Remover." *Journal of Clinical Periodontology* 30, no. 2: 138–144. <https://doi.org/10.1034/J.1600-051X.2003.00114.X>.
- Del Rey, Y. C., P. D. Rikvold, K. K. Johnsen, and S. Schlafer. 2023. "A Fast and Reliable Method for Semi-Automated Planimetric Quantification of Dental Plaque in Clinical Trials." *Journal of Clinical Periodontology* 50, no. 3: 331–338.
- Doi, K., C. Yoshiga, R. Kobatake, M. Kawagoe, K. Wakamatsu, and K. Tsuga. 2021. "Use of an Intraoral Scanner to Evaluate Oral Health." *Journal of Oral Science* 63, no. 3: 292–294. <https://doi.org/10.2334/JOSNUSD.21-0048>.
- Fasoulas, A., E. Pavlidou, D. Petridis, M. Mantzorou, K. Seroglou, and C. Giaginis. 2019. "Detection of Dental Plaque With Disclosing Agents in the Context of Preventive Oral Hygiene Training Programs." *Heliyon* 5, no. 7: e02064. <https://doi.org/10.1016/j.heliyon.2019.e02064>.
- Gallagher, I. H. C., S. J. Fussell, and T. W. Cutress. 1977. "Mechanism of Action of a Two-Tone Plaque Disclosing Agent." *Journal of Periodontology* 48, no. 7: 395–396. <https://doi.org/10.1902/JOP.1977.48.7.395>.
- Giese-Kraft, K., K. Jung, N. Schlueter, K. Vach, and C. Ganss. 2022. "Detecting and Monitoring Dental Plaque Levels With Digital 2D and 3D Imaging Techniques." *PLoS One* 17, no. 2: e0263722. <https://doi.org/10.1371/JOURNAL.PONE.0263722>.
- Gkavela, G., P. E. Nørrisgaard, and C. Rahiotis. 2024. "Level of Agreement Between Plaque Detection With Clinical Assessment and Assessment on Intraoral Scanner." *Dentistry Journal* 12, no. 12: 395. <https://doi.org/10.3390/dj12120395>.
- Jakovovics, N. S., S. D. Goodman, L. Mashburn-Warren, G. P. Stafford, and F. Cieplik. 2021. "The Dental Plaque Biofilm Matrix." *Periodontology* 2000 86, no. 1: 32–56. <https://doi.org/10.1111/PRD.12361>.
- Jung, K., K. Giese-Kraft, M. Fischer, K. Schulze, N. Schlueter, and C. Ganss. 2022. "Visualization of Dental Plaque With a 3D-Intraoral-Scanner-A Tool for Whole Mouth Planimetry." *PLoS One* 17, no. 10: e0276686. <https://doi.org/10.1371/JOURNAL.PONE.0276686>.
- Jung, K., K. Giese-Kraft, M. A. Schlenz, B. Wöstmann, and C. Ganss. 2024. "Digital Plaque Monitoring: An Evaluation of Different Intraoral Scanners." *Journal of Dentistry* 145: 104978. <https://doi.org/10.1016/J.JDENT.2024.104978>.
- Kihara, H., W. Hatakeyama, F. Komine, et al. 2020. "Accuracy and Practicality of Intraoral Scanner in Dentistry: A Literature Review." *Journal of Prosthodontic Research* 64, no. 2: 109–113. <https://doi.org/10.1016/J.JPOR.2019.07.010>.
- Kottner, J., L. Audigé, S. J. Brorson, et al. 2011. "Guidelines for Reporting Reliability and Agreement Studies (GRRAS) Were Proposed." *Journal of Clinical Epidemiology* 64, no. 1: 96–106. <https://doi.org/10.1016/J.JCLINEPI.2010.03.002>.
- Kuralt, M., and A. Fidler. 2021. "Assessment of Reference Areas for Superimposition of Serial 3D Models of Patients With Advanced Periodontitis for Volumetric Soft Tissue Evaluation." *Journal of Clinical Periodontology* 48, no. 6: 765–773. <https://doi.org/10.1111/JCPE.13445>.
- Kuralt, M., and A. Fidler. 2022. "A Novel Computer-Aided Method for Direct Measurements and Visualization of Gingival Margin Changes." *Journal of Clinical Periodontology* 49, no. 2: 153–163. <https://doi.org/10.1111/JCPE.13573>.
- Kuralt, M., R. Gašperšič, and A. Fidler. 2020. "3D Computer-Aided Treatment Planning in Periodontology: A Novel Approach for Evaluation and Visualization of Soft Tissue Thickness." *Journal of Esthetic and Restorative Dentistry* 32, no. 5: 457–462. <https://doi.org/10.1111/JERD.12614>.
- La Rosa, G. R. M., I. Chapple, R. Polosa, and E. Pedullà. 2023. "A Scoping Review of New Technologies for Dental Plaque Quantitation: Benefits and Limitations." *Journal of Dentistry* 139: 104772. <https://doi.org/10.1016/J.JDENT.2023.104772>.
- Lang, N. P., B. R. Cumming, and H. Löe. 1973. "Toothbrushing Frequency as It Relates to Plaque Development and Gingival Health." *Journal of Periodontology* 44, no. 7: 396–405. <https://doi.org/10.1902/JOP.1973.44.7.396>.
- Lee, S. J., S. W. Kim, J. J. Lee, and C. W. Cheong. 2020. "Comparison of Intraoral and Extraoral Digital Scanners: Evaluation of Surface Topography and Precision." *Dentistry Journal* 8, no. 2: 52. <https://doi.org/10.3390/DJ8020052>.
- Li, Q., K. Rycaj, X. Chen, and D. G. Tang. 2015. "Cancer Stem Cells and Cell Size: A Causal Link?" *Seminars in Cancer Biology* 35: 191–199. <https://doi.org/10.1016/J.SEMCANCER.2015.07.002>.
- Lin, W. Q., C. Y. Pan, P. H. Chen, C. Liu, C. C. Te Hung, and T. H. Lan. 2024. "Trueness of Intraoral Scanning for Different Tooth-Size Arch-Length Deficiencies." *Journal of Dental Sciences* 19, no. 1: 397–403. <https://doi.org/10.1016/J.JDS.2023.08.006>.
- Lobene, R. R., S. M. Mankodi, S. G. Ciancio, R. A. Lamm, C. H. Charles, and N. M. Ross. 1989. "Correlations Among Gingival Indices." *Journal of Periodontology* 60, no. 3: 159–162. <https://doi.org/10.1902/JOP.1989.60.3.159>.
- Lobene, R. R., P. M. Soparkar, and M. B. Newman. 1982. "Use of Dental Floss. Effect on Plaque and Gingivitis." *Clinical Preventive Dentistry* 4, no. 1: 5–8.
- Lütkenhöner, B., M. Hoke, and C. Pantev. 1985. "Possibilities and Limitations of Weighted Averaging." *Biological Cybernetics* 52, no. 6: 409–416. <https://doi.org/10.1007/BF00449599>.
- Rusinkiewicz, S. 2004. "Estimating Curvatures and Their Derivatives on Triangle Meshes." Proceedings – 2nd International Symposium on 3D Data Processing, Visualization, and Transmission. 3DPVT 2004, 486–493. <https://doi.org/10.1109/TDPVT.2004.1335277>.
- Rustogi, K. N., J. P. Curtis, A. R. Volpe, J. H. Kemp, J. J. McCool, and L. R. Korn. 1992. "Refinement of the Modified Navy Plaque Index to Increase Plaque Scoring Efficiency in Gumline and Interproximal Tooth Areas." *Journal of Clinical Dentistry* 3, no. Suppl C: C9–C12. <https://europepmc.org/article/med/1306676>.
- Schmidt, L. R., A. Binder, R. Kampschilte, et al. 2022. "Accuracy of Digital Impression Taking With Intraoral Scanners and Fabrication of CAD/CAM Posts and Cores in a Fully Digital Workflow." *Materials (Basel)* 15, no. 12: 4199.
- Schober, P., and L. A. Schwarte. 2018. "Correlation Coefficients: Appropriate Use and Interpretation." *Anesthesia and Analgesia* 126, no. 5: 1763–1768. <https://doi.org/10.1213/ANE.0000000000002864>.
- Silness, J., and H. Löe. 1964. "Periodontal Disease in Pregnancy. II. Correlation Between Oral Hygiene and Periodontal Condition." *Acta Odontologica Scandinavica* 22, no. 1: 121–135. <https://doi.org/10.3109/00016356408993968>.
- Turesky, S., N. D. Gilmore, and I. Glickman. 1970. "Reduced Plaque Formation by the Chloromethyl Analogue of Vitamin C." *Journal of Periodontology* 41, no. 1: 41–43. <https://doi.org/10.1902/JOP.1970.41.41.41>.
- Vág, J., Z. Nagy, B. Simon, et al. 2019. "A Novel Method for Complex Three-Dimensional Evaluation of Intraoral Scanner Accuracy." *International Journal of Computerized Dentistry* 22, no. 3: 239–249.

Volgenant, C. M. C., M. Fernandez y Mostajo, N. A. M. Rosema, F. A. van der Weijden, J. M. ten Cate, and M. H. van der Veen. 2016. "Comparison of Red Autofluorescing Plaque and Disclosed Plaque—A Cross-Sectional Study." *Clinical Oral Investigations* 20, no. 9: 2551–2558. <https://doi.org/10.1007/S00784-016-1761-Z>.

Winkler, J., and N. Gkantidis. 2020. "Trueness and Precision of Intraoral Scanners in the Maxillary Dental Arch: An In Vivo Analysis." *Scientific Reports* 10, no. 1: 1–11. <https://doi.org/10.1038/s41598-020-58075-7>.

### Supporting Information

Additional supporting information can be found online in the Supporting Information section. **Figure S1:** Calibration exercise for the assessment of clinical parameters. **Table S1:** Inclusion and exclusion criteria. **Table S2:** GRRAS checklist for reporting of studies of reliability and agreement. **Table S3:** Differences in VPI and AVPI between extraoral and intraoral scanning, as part of the ex vivo validation protocol. **Table S4:** Differences in VPI and AVPI between extraoral and intraoral scanning, as part of the in vivo validation protocol. **Table S5:** Outcomes of the exploratory pairwise comparisons (*p*-values) between DDP and TDP scores (assessed using the TMQHPII) for VPI using the Mann–Whitney U test. **Table S6:** Outcomes of the exploratory pairwise comparisons (*p*-values) between DDP and TDP scores (assessed using the TMQHPII) for AVPI using the Mann–Whitney U test. **Table S7:** Diagnostic validity of the TMQHPII and VPI.